Emerging dynamic regimes and tipping points from finite empirical principles

Sergio Cobo-López[1,2,3], Matthew Witt[1,4], Lucas J. Carbajal[5], Forest L. Rohwer[1,2], and Antoni Luque[1,5]

[1] *Viral Information Institute, San Diego State University, San Diego, CA 92182, USA*

[2] *Department of Biology, San Diego State University, San Diego, CA 92182, USA*

[3] *Departament d'Enginyeria Química, Universitat Rovira i Virgili, Tarragona, Catalonia, Spain*

[4] *Department of Physics, San Diego State University, San Diego, CA 92182*

[5] *Department of Biology, University of Miami, 1301 Memorial Dr, Coral Gables, FL 33155, USA*

[6] *Department of Mathematics and Statistics, San Diego State University,San Diego, CA 92182, USA*

[7] *Computational Science Research Center, San Diego State University, San Diego, CA 92182, USA*

December 20, 2024

Abstract

All dynamical systems are transient. The dynamics of our world at biogeochemical, ecological, and astronomical scales exist in a transient state because the Earth, Sun, and universe are evolving toward thermodynamic equilibrium. However, predicting the tipping points associated with major dynamical shifts in these systems remains a significant challenge. Here, we introduce a new theoretical framework to predict tipping points. Our approach builds on two empirical principles: Observations occur over a finite time, and changes are perceptible when system variations are substantial relative to reference values. As a consequence, processes governing the dynamics of a system can become inactive over an observation time, and tipping points are reached when the processes switch off or on. The two principles were encoded mathematically, defining dynamic weights: contributions relative to reference values of the dynamic processes to the rate-of-change of agents in the system for a finite observational time. Operationally, processes were considered active if their weights were above a critical threshold. Tipping points were defined as reaching critical thresholds that activated or inactivated processes. This Finite Observational Dynamics Analysis Method (FODAM) predicted that a system with n underlying dynamic processes could display 2^n different dynamic regimes. However, the structure of regimes depend on the observational time. The tipping points predicted the conditions for regime shifts. The application of FODAM was illustrated with a Lotka-Volterra predator-prey model featuring the interaction of bacteria and bacteriophage.

The error of the method was analyzed and discussed. Also, Colab notebook was developed and deployed online to facilitate the application of the method to other systems. We conclude the article by discussing how our new approach bridges prior frameworks describing tipping point dynamics and critical transitions. We also outline the application of the method to empirical data to predict tipping points in complex systems.

Introduction

All dynamical systems in nature display transient dynamics, where a system experiences a regime shift after crossing a tipping point or critical threshold (Scheffer 2009; Strogatz 2015). The emergence of marine photosynthetic bacteria 2.5 billion years ago triggered a transition from low to high oxygen in the atmosphere (Margulis and Sagan 1997; Lyons et al. 2014), and the disruption of the thermal-haline marine current in the Atlantic 12000 years ago (the Younger-Dryas period) reversed the recovery from the last Glaciation period (Scheffer 2009; Cheng et al. 2020). Even the periodic dance of planets around the Sun is predicted to derive into a chaotic dynamic in two billion years, likely leading to a collision between Earth, Mars, Venus, or Mercury (Laskar and Gastineau 2009; Hayes 2007), although by then the Sun will have expanded as a red star and will likely engulf our beloved rocky planets (Schroder and Smith 2008; De et al. 2023). Transient dynamics are, thus, unavoidable in the study of natural systems. However, it is very difficult to predict the tipping points causing a regime shift(Seekell 2016; Scheffer et al. 2009).

A common approach to studying transient dynamics is to assume that the system is stable in the vicinity of the equilibrium (Panahi et al. 2023). However, systems must be often addressed while in motion rather than equilibrium, for example, during a pandemic or an atmospheric event. Theoretically, the use of two-timing approaches (Cole and Kevorkian 1963; Kevorkian 1966; Kevorkian and Cole 1981) can help separate different timescale mechanisms, although, in practice, this method assumes asymptotic time for the slow process. The standard approach, in that case, is to model the system, for example, using differential equations and integrate them numerically to obtain the trajectories in the regions of interest (Bashkirtseva and Ryashko 2018; Cairns et al. 2009; Cushing et al. 1998; Roach et al. 2017; Rabinovich et al. 2006; Rinaldi and Scheffer 2000). Fitting these models to empirical data provides parameter values that can reproduce the transient dynamics and can be used to interpret experiments and forecasts (Cairns et al. 2009). This approach, however, requires an exhaustive exploration of the parameter space, and the complexity of the system can hinder the ability to predict the potential existence of regime shifts (Roach et al. 2017). Lastly, some empirical approaches have made significant progress in predicting tipping points using machine learning (Oro et al. 2023) or statistical time series analysis. These approaches include the analysis of mean rates of state variables (Pedersen et al. 2020), the application of conditional heteroskedasticity to ecological systems (Seekell et al. 2011, 2012, 2013; Pedersen et al. 2020), or the

identification of early-warning signals through resilience analysis (Scheffer et al. 2009; Ditlevsen and Ditlevsen 2023; Bury et al. 2021.) However, unlike the study of asymptotic dynamics or equilibria, a quantitative framework to classify and investigate transient dynamics mechanistically is still under development (Strogatz 2015; Hastings et al. 2018).

Regime shifts in transient dynamics can range from gradual to dramatic and can be triggered by large to small changes in internal or external variables (Hastings et al. 2018; Scheffer 2009). In general, during transient dynamics, the system variables can show a gradual or minor drift followed by a sudden and extensive change (Rocha et al. 2018). However, the study of dynamical systems is grounded on methods that rely on asymptotic equilibria and stability (Strogatz 2015). To facilitate the characterization and prediction of regime shifts and the transient nature of physical systems, we propose a framework that measures the weight of individual processes in the dynamics of a system. The approach builds on two assumptions. First, a process in a dynamical system is considered active if it changes substantially within a finite observational timescale that depends on the specific study of interest. Second, the substantial change is normalized to a reference value of the variable impacted by the process. Note that the term active in this context refers to the contribution of the process to the dynamics. The results section outlines how these assumptions can be applied to obtain tipping points or critical concentrations associated with different regimes in a dynamical system. We illustrate the application of the general method using a classic predator-prey system modeled by a Lotka-Volterra dynamical system. To make the choice of conditions more specific, we focused on the interaction of bacteria and their associate viruses (called bacteriophages or phages). The approach identified 16 (2^4) dynamic regimes depending on which processes were active within the observational timescale of the study. The critical thresholds obtained were also applied to investigate the resilience of the system to perturbations, showing a dramatically different response when perturbations crossed these values. The discussion section further elaborates on how to use this approach to investigate real systems with many variables. We also elaborated on how the assumptions lead to bounded theoretical errors that can be reduced based on the needed experimental resolution analyzed the error in the case study presented here.

Results

General results of the Finite Observational Dynamics Analysis Method (FODAM)

Prediction of dynamic regimes and tipping points The finite observational principle implies that the observational time Δt^{obs} and the significant change on a dynamic agent ΔA_i^{obs} (Fig. 1), are finite for every observer. The application of the observational principle to a dynamical system

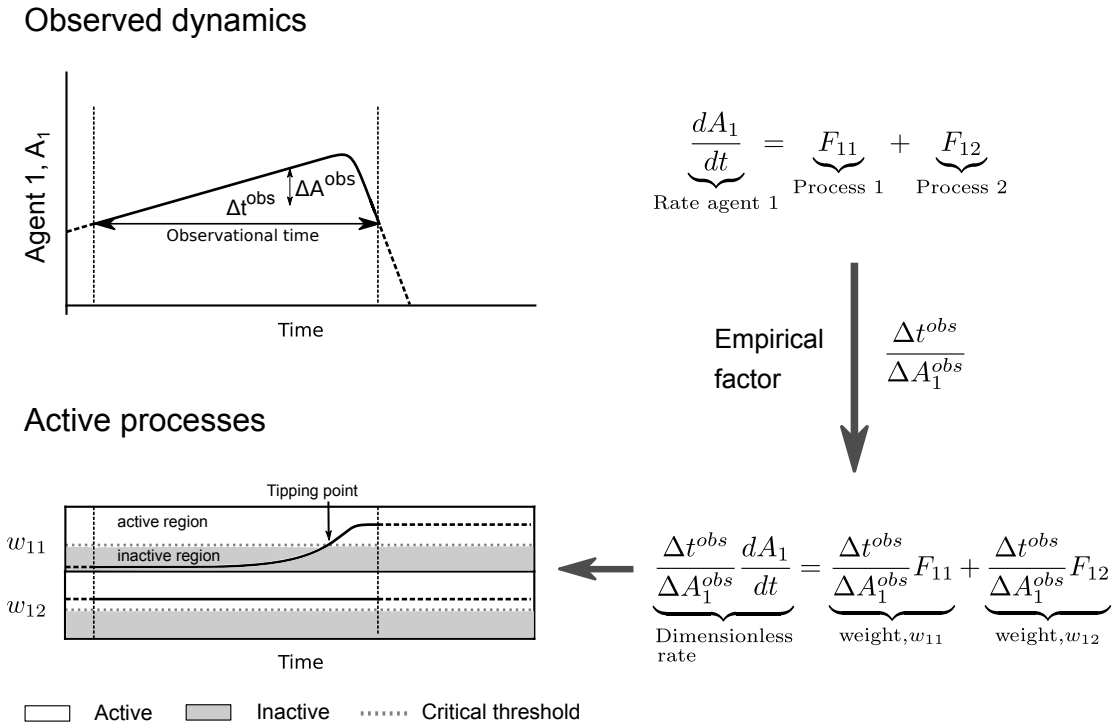

$$\underbrace{\frac{dA_1}{dt}}_{\text{Rate agent 1}} = \underbrace{F_{11}}_{\text{Process 1}} + \underbrace{F_{12}}_{\text{Process 2}}$$

$$\underbrace{\frac{\Delta t^{obs}}{\Delta A_1^{obs}}\frac{dA_1}{dt}}_{\text{Dimensionless rate}} = \underbrace{\frac{\Delta t^{obs}}{\Delta A_1^{obs}}F_{11}}_{\text{weight},w_{11}} + \underbrace{\frac{\Delta t^{obs}}{\Delta A_1^{obs}}F_{12}}_{\text{weight},w_{12}}$$

Figure 1: **FODAM analysis**. Application of FODAM to a system comprising an agent A_1 whose dynamics are governed by processes F_{11} and F_{12}. The finite observational principle sets an observational time Δt^{obs} and a significant change ΔA_1^{obs}. Multiplying the dynamic equation by the empirical factor $\frac{\Delta t^{obs}}{\Delta A_1^{obs}}$ yields a dimensionless system with weights w_{11} and w_{12}. The processes F_{11} and F_{12} are active if the weights are equal or larger than 1, and inactive otherwise. $w_{1j} = 1$ is the critical threshold and the system reaches a tipping point if it crosses any critical threshold.

containing N agents yields the rescaled dimensionless system:

$$\sum_{i=1}^{N} \frac{\Delta t^{obs}}{\Delta A_i^{obs}} \frac{dA_i}{dt} = \sum_{j=1}^{M_i} w_{ij}, \quad \text{where} \quad w_{ij} = \frac{\Delta t^{obs}}{\Delta A_i^{obs}} F_{ij}. \tag{1}$$

Here M_i is the number of processes impacting the rate of change of agent A_i, F_{ij} is the j-th process impacting the i-th agent, and w_{ij} is the weight of process F_{ij}. F_{ij} is an active process if:

$$|w_{ij}| \geq 1\,. \tag{2}$$

The condition above implies that F_{ij} induces a change in A_i of the same order of magnitude or higher as the significant observational change, ΔA_i^{obs}, within the observational time, Δt^{obs}. In other words, F_{ij} is an active process because it has a significant empirical impact in the dynamic of A_i. (2) sets a critical threshold of order one, and the corresponding values of $A_i^{\star}$ define the tipping point of A_i (Fig. 1). Within FODAM, the dynamics of the system are thus defined only by the active processes at time t. Each combination of active processes defines a different dynamic regime. Thus, given a system with $M = \Sigma_i M_i$ processes, there are 2^M dynamic regimes. The subset of active processes generates an attractor that drives the trajectory of the dynamic regime. This attractor can lead the system to crossing other tipping points, thus, activating or inactivating other processes and defining a new dynamic regime with a different attractor. A system is stable or quasi-stable if it remains in the same dynamic regime within an observational timescale.

Error of the approximated dynamic regimes. Applying the condition Eq. (2) to the rescaled dynamical system Eq. (1) yields a simplified dynamical system comprising only the active processes in a dynamic regime:

$$\frac{\Delta t^{obs}}{A_i} \frac{dA_i}{dt} \approx \sum_{j=1}^{M_i^{\mathcal{O}_1}(t)} w_{ij}^{\mathcal{O}_1}\,. \tag{3}$$

Here, $M_i^{\mathcal{O}_1}(t)$ is the number of active processes of first order at time t. The simplified dynamics in Eq.(3) can be used to estimate the error of the critical threshold, Eq.(2): if the error is too high, the critical threshold needs to be lower than one.

Lotka-Volterra as case study

To illustrate the characterization and prediction of dynamic regimes and tipping points, FODAM was applied to a classic Lotka-Volterra model in the context of bacteria as the prey and phage as the predator.

Dynamic regimes and tipping points of the case study The Lotka-Volterra system was defined by two agents (see Fig. 2): Bacteria or prey ($B(t)$) and phage or predator ($P(t)$). The two

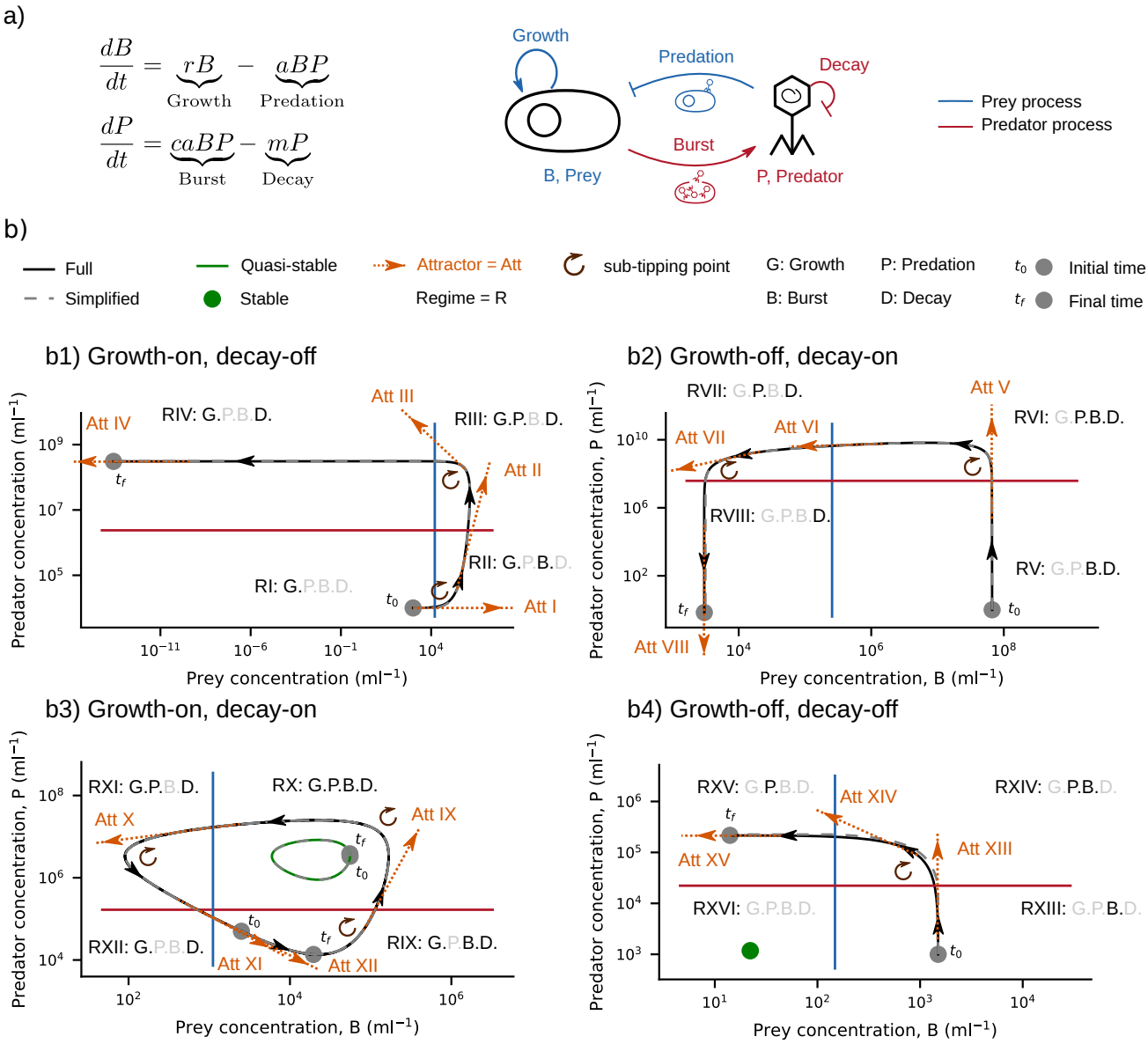

Figure 2: **FODAM application to a Lotka-Volterra system: phase diagrams of the dynamic regimes**. **a)** Lotka-Volterra equations for a phage-bacterial system. **b)** Phase diagrams of the 2^4 =16 regimes predicted by FODAM. The concentration of predator (phage) is shown as a funcion of the concentration of prey (bacteria). All phase diagrams are displayed on a logarithmic scale and distributed in four categories depending on whether growth and decay are active or inactive. Solid black lines correspond to the full model, while gray dashed lines represent the simplified model with the active terms in each regime. Orange dashed lines indicate the attractors of a regime, and green lines and dots represent quasi-stable and stable dynamics. Vertical (red) and horizontal (blue) lines indicate the critical thresholds B_c and P_c respectively, marking the tipping points between regimes. Roman numbers label dynamic regimes, followed by the initial letter of active processes in black and inactive processes in pale gray. Brown circular arrows show sub-tipping points, where the trend of an agent changes. t_0 and t_f indicate the initial and final times of the simulation. **b1)** Transition across Regimes I to IV with growth (G.) active and decay (D.) inactive, **b2)** Transition across regimes V to VIII with growth inactive, decay active, **b3)** Transition across regimes IX to XII (including quasi-stable regime X) with growth and decay active, and **b4)** Transition across regimes XIII to XV and regime XVI. Regime XVI corresponds to no active mechanism and is not accessible from any other regime.

processes impacting the prey population were the bacterial growth ($F_g = rB$), and the predation of phage on bacteria ($F_p = -aPB$). The two processes impacting the predator population were the burst ($F_b = caPB$), and the phage decay ($F_d = -mP$) (Fig. 2). The observational time, Δt^{obs}, was defined by the parameter τ, which took different values. The reference values for the signicant observational change were $\Delta A_1^{obs} = B(t)$ and $\Delta A_2^{obs} = P(t)$, the values of each variables at each time t. Using the dynamical values as reference values facilitates the analysis of the populations if their concentrations change orders of magnitude, which is common in these systems. The application of Eq. (1) yields in the following transformed Lotka-Volterra system with explicit weights for each process:

$$\begin{aligned} \frac{\tau}{B}\frac{dB}{dt} &= \underbrace{\tau\, r}_{growth} - \underbrace{\tau\, a\, P}_{predation} \\ \frac{\tau}{P}\frac{dP}{dt} &= \underbrace{\tau\, c\, a\, B}_{burst} - \underbrace{\tau\, m}_{decay} \,. \end{aligned} \tag{4}$$

The four weights are $w_g = \tau\, r$ (bacterial growth), $w_p = \tau\, a\, P$ (bacterial predation), $w_b = \tau\, c\, a\, B$ (phage burst), and $w_d = \tau\, m$ (phage decay). Note that bacterial growth and phage decay processes are constant and proportional to the observational time, τ. There is no dynamic tipping point associated to their activation, but the value of τ defines whether they are active or not. Bacterial predation and phage burst are instead functions of the dynamic variables, $P(t)$ and $B(t)$, respectively. As a result, they define tipping points $P_c^{predation}$ and B_c^{burst}, that can activate or inactivate the processes. Applying the first-order condition for the weights Eq. (2), yielded the critical values:

$$\begin{aligned} P_c^{predation} &= \frac{1}{\tau\, a} \\ B_c^{burst} &= \frac{1}{\tau c a} \,. \end{aligned} \tag{5}$$

Since the Lotka-Volterra system contains four processes, $M = 4$, FODAM predicts $2^4 = 16$ different dynamic regimes.

The attractors and asymptotic stability for each of the 16 regimes were obtained theoretically (Tables S1-S4). The analysis showed only two potential quasi-stable regimes (green lines in Fig. 2): Regime XVI (all processes inactive) and Regime X (all processes active). The remaining 14 regimes displayed attractors that either drove the system away from the given regime by crossing tipping points (Regimes I-III, V-VII, IX, XI-XIV) or led to the effective extinction of one of the agents (Regimes IV, VIII, and XV). To visualize these general results, the Lotka-Volterra model was parametrized using four sets of values from isolated phage-bacteria systems as well as phage-bacteria communities and different observational times (Table S5). These values allowed the numerical simulation of the full model, thresholds, tipping points, and the approximated dynamics, recovering the 16 predicted dynamic regimes discussed above as illustrated in Fig. 2b. The regimes were grouped in four categories based on whether the processes with constant weights (bacterial growth and phage decay) were active or not: growth-on.decay-off (Fig. 2b1 and Table S1), growth-

off.decay-on (Fig. 2b2 and Table S2), growth-on.decay-on (Fig. 2b3 and Table S3), and growth-off.decay-off (Fig.e 2b4 and Table S4).

The scenario growth-on.decay-off (Figure 2 b1 and Table S1) was obtained for typical values of the laboratory model systems *E. coli* and phage T4 (Table S5). The observation timescale was set to $\Delta t^{obs} \sim 14$ hours, a reasonable value for a single-day experiment (Figure 3). The bacterial growth rate was $r = 0.9$ h^{-1} with an associated weight $w_{11} = 126$, that is, active. The phage decay rate was $m = 1.5 \cdot 10^{-3}$ h^{-1}, with an associated weight $w_{22} = 0.21$, that is, inactive. The tipping point for the burst process was $B_c = 2.6 \cdot 10^4$ cells/ml, and for the bacterial predation was $P_c = 1.3 \cdot 10^6$ phages/ml (Eq 5). The initial concentrations were chosen below these tipping points, respectively, $B(0) = 10^3$ cells/ml and $P(0) = 10^4$ phages/ml, which are reasonable values for the initial conditions of phage-bacteria laboratory experiments. This set the system in Regime I with just the bacterial growth process active. The theoretical attractors for this scenario (Table S1) predicted that the system would cross first the tipping point for the bacterial concentration activating the burst phage process (Regime II: growth and burst), which occurred at time 1.06 hours in the simulation. Then the attractor associated to the burst of phage was predicted to cross the tipping point associated with the critical phage concentration activating the bacterial predation (Regime III: growth, predation, and burst), which occurred at time 7.49 hours. The attractor for Regime III predicted an increase of phage leading to a much larger predation effect than growth, thus, reducing the bacteria population and crossing back the tipping point for the bacterial concentration associated to phage burst, which occurred at time 9.90 hours. This led to Regime IV (growth, predation) and the effective bacteria extinction in the system. The results in Figures 2 b1 and 3 confirmed the theoretical predictions of the dynamic regimes for this scenario, underpinning the importance of incorporating the finite observational time and significant observational change when analyzing dynamical systems and identifying tipping points.

The same strategy was followed for the other three scenarios illustrated, respectively, in Figs. 2b2, 2b3, and 2b4. The explicit time series was investigated in Figs. 4, 5 and in Figs. S1 and S2. An important observation was determining the conditions that would lead to a quasi-stable dynamic. Besides the trivial case of all processes being inactive, the growth-on.decay-on scenario trapped in Regime X (green phase diagram in Fig 2 2c) also displays a quasi-stable behavior because it does not cross any critical threshold. FOMAD predicts quasi-stability or stability for systems that do not cross critical thresholds, which is more constraining than the traditional asymptotic analysis. Note also that Regime X precisely corresponds to the original full Lotka-Volterra equations.

Error of the simplified model in the case study. We use the relative error to measure the error of the adaptive model, as shown in Figures (3 d, 4 d , and 5 d).

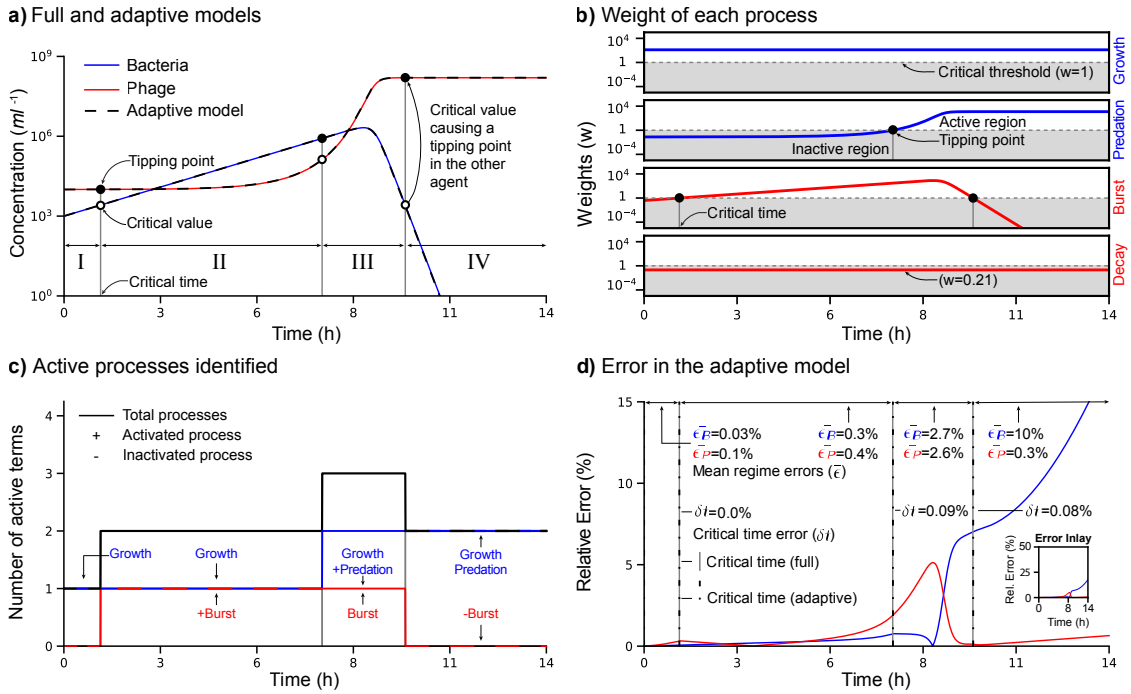

Figure 3: **Predicted scenario with active growth and inactive decay. a)** Dynamics of the bacteria (blue line) and phage (red line) populations using the full model. The parameters were r $= 0.9$ h^{-1} (growth rate constant), a$= 3.0 \cdot 10^{-8}$ ml/h (infection rate constant), c $= 150$ (burst size), m $= 2.8 \cdot 10^{-3}$ h $^{-1}$ (decay rate constant). The open circles highlight the critical values of a population, which occur at the critical threshold, when the weight of the process is one (see panel b) and leads to a tipping point in the other agent (black circle). The vertical lines indicate the critical times between transient dynamic regimes, numbered using Roman numerals. The horizontal arrows indicate the duration of the regime. The dashed lines are the populations obtained from the adaptive model, with only active processes (see panel c). **b)** Weights of each process in the dynamics. The right axis lists the name of the process. Blue processes are associated with bacteria, and red with phages. The dashed horizontal line indicates the critical threshold ($w = 1$). The white regions indicate when a process is active, and the grey one when it is inactive. **c)** The number of active processes is plotted for each agent following the colors in panel a. The labels indicate the processes active in each regime. The black line corresponds to the total number of active processes. **d)** Errors in the adaptive model for both populations. The vertical lines display the critical times for the full model (solid grey) and the adaptive model (dashed dot). The critical time relative error (δt) is displayed at each transition point. The mean relative errors for the bacteria ($\bar{\epsilon}_B$) and phage populations ($\bar{\epsilon}_P$) are displayed at each regime. The error inlay displays the relative error percentage vs time above the y-axis limit of 15 % .

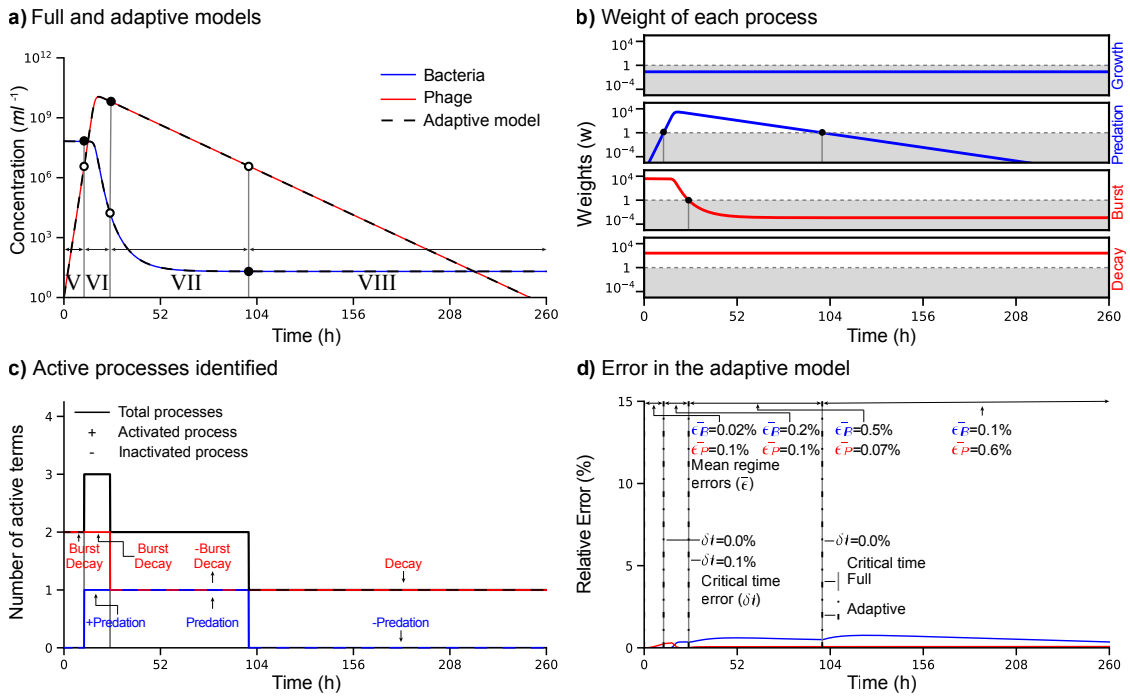

Figure 4: **Predicted scenario with inactive growth and active decay. a)** Dynamics of the bacteria (blue line) and phage (red line) populations using the full model. The parameters were r $= 3.2 \cdot 10^{-5}$ h^{-1} (growth rate constant), a $= 1.0 \cdot 10^{-10}$ ml/h (infection rate constant), c $= 225$ (burst size), m $= 0.1$ h^{-1} (decay rate constant). The transient dynamic regimes are numbered by Roman numerals, and duration shown by horizontal line. The dashed lines are the populations obtained from the adaptive model, only consisting of active processes. **b)** Weights of each process in the dynamics. Blue processes are associated with bacteria, and red with phages. **c)** The number of active processes is plotted for each agent following the colors in panel a. The labels indicate the processes active in each regime. The black line corresponds to the total number of active processes. **d)** Errors in the adaptive model for both populations. The vertical lines display the critical times for the full model (solid grey) and the adaptive model (dashed dot). The critical time relative error (δt) is displayed at each transition point. The mean relative errors for the bacteria ($\bar{\epsilon_B}$) and phage populations ($\bar{\epsilon_P}$) are displayed at each regime.

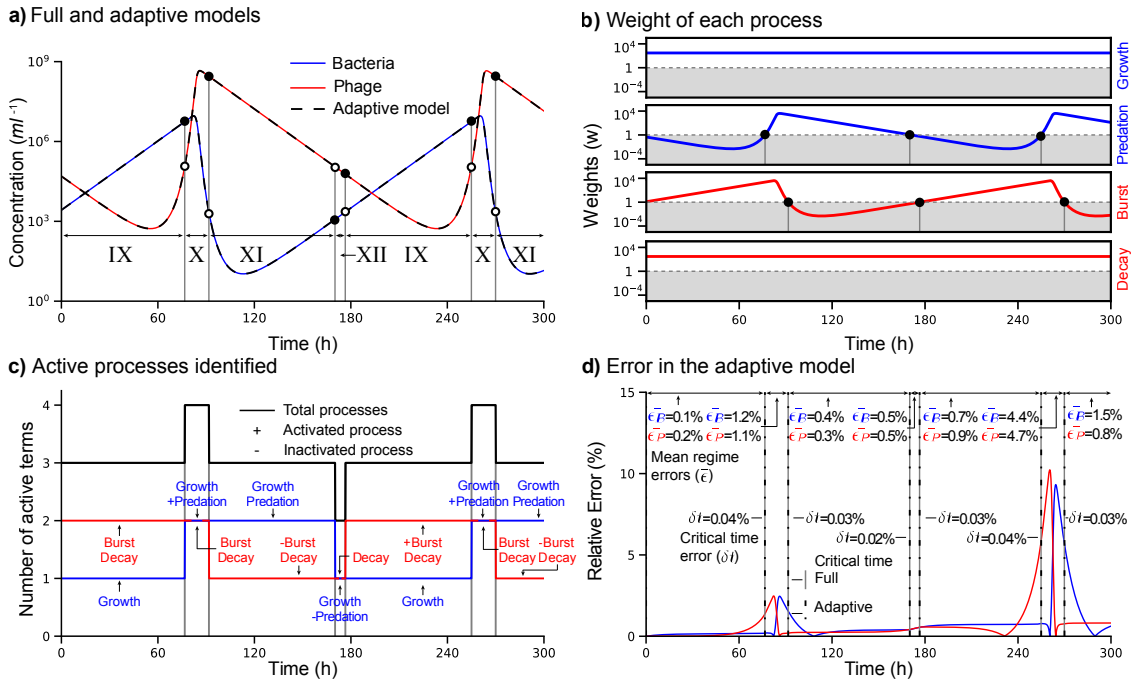

Figure 5: **Predicted scenario with active growth and decay.** **a)** Dynamics of the bacteria (blue line) and phage (red line) populations using the full model. The parameters were r = 0.1 h^{-1} (growth rate constant), a= $3.0 \cdot 10^{-9}$ ml/h (infection rate constant), c = 50 (burst size), m = 0.1 h^{-1} (decay rate constant). The transient dynamic regimes are numbered by Roman numerals, and duration shown by horizontal line. The dashed lines are the populations obtained from the adaptive model, only consisting of active processes. **b)** Weights of each process in the dynamics. Blue processes are associated with bacteria, and red with phages. **c)** The number of active processes is plotted for each agent following the colors in panel a. The labels indicate the processes active in each regime. The black line corresponds to the total number of active processes. **d)** Errors in the adaptive model for both populations. The critical time relative error (δt) is displayed at each transition point. The mean relative errors for the bacteria ($\bar{\epsilon_B}$) and phage populations ($\bar{\epsilon_P}$) are displayed at each regime.

Discussion

Our results show that given any dynamical model, only the active processes within an observation timescale Δt^{obs} drive their behavior, while inactive processes can be neglected. Therefore, a simplified model consisting only of those active processes can accurately describe the dynamics of a system. A consequence of this result is that even a relatively small system consisting of only four dynamic processes actually comprises 2^4 dynamic regimes, each defined by the corresponding active terms. Dynamic processes are activated and inactivated endogenously, moving the system across different regimes in the four scenarios described in the main text. We define the tipping points as the critical concentrations of phages and bacteria that activate and inactivate processes. Within FODAM, the tipping points and the number of dynamics in a system can be calculated a priori. Neglecting specific, well-defined processes can lead to seemingly paradoxical situations. Consider, for instance, dynamic regime II in the first scenario discussed: the phage burst process was active, but the bacterial predation was not (Fig. 3). As counterintuitive as it looks, the simplified model recovered the full dynamic with great accuracy. This result has an interesting implication: it would be impossible to determine from statistical inference that the dramatic increase in phage was related to the bacterial growth and that this growth would be related to the subsequent bacterial extinction. Fortunately, the findings presented here pave the way for assessing this limitation. If one can propose plausible processes governing the dynamics of a system, it is possible to extract the conditions under which they will impact the dynamic. Likewise, it will be possible to produce a simplified model with active processes to assess the accuracy of its prediction.

In the case investigated here, the simplified model led to high accuracies compared to the full model (Figures 3 , 4 , and 5). This was partially because inactive terms had weights far below one (see Eqs. 1, 2 and Supplementary Materials). However, the upper bound of the error could be reduced by considering lower-order thresholds. Note that this is not a consequence of the relative simplicity of the model considered here since the mathematical framework is independent of the system. This generality makes the application of FODAM to more complex problems very promising. The Colab tool attached to this manuscript (see Methods section) already provides many opportunities for the curious reader. However, we can readily imagine that FODAM could work as a decluttering tool for very large models, removing terms that are always inactive within the corresponding timescale.

In short, FODAM is a pragmatic approach to forecasting tipping points and regime shifts in real systems. The weights of processes act as early warning signals as they approach their tipping points, in a similar way as the resilience does in other approaches (Scheffer 2009; Folke et al. 2010; Ditlevsen and Ditlevsen 2023; Bury et al. 2021). However, within FODAM, critical transitions occur when dynamical terms become active or inactive. Each regime out of the 16 existing ones described in our case study is characterized by a different attractor. As the system moves to an

attractor, it may activate new terms, shift the dynamic, and move to a new attractor. Thus, the transient dynamics relevant to the study display multistability, although the system would not have been characterized as multistable in the classical asymptotic approach. The activation of dynamic terms changes the energy landscape and leads to a regime shift. These activations can be due to internal (dynamic variables) or external changes (observational timescale). FODAM provides a basic protocol to forecast regime shifts in real systems: obtain data of the system for a time shorter than the observational timescale; assess the weights of the plausible processes; determine active ones and tipping points; predict dynamic shifts; be prepared for the shift or act to prevent it. The Colab notebook attached to this manuscript (`https://colab.research.google.com/github/luquelab/dynamics/blob/main/dynamic_regimes.ipynb`) allows for potential applications of FODAM to other models defined by the users.

Methods

FODAM for Lotka-Volterra equations

The application of FODAM to Eq. 4 consisted of two steps: 1) divide each net rate by the reference values, obtaining the net rate per capita, and 2) multiply the equation by the observational timescale, τ. These two steps yielded a dimensionless dynamical system. Each transformed dimensionless process was defined as the dynamic weight of that process. Constant weights defined critical timescales when their weight values were of order one. Weights that depended on dynamic variables defined critical concentration thresholds when the dynamic variables led to weight values of order one.

Classic stability analysis

The four processes defining the Lotka-Volterra model, Eq. 4, generated 16 (2^4) dynamic regimes or sub-models defined by the presence or absence of processes in the equations. For each sub-model, the equilibrium was obtained by setting the equation rates to zero and extracting the fixed points. A valid equilibrium existed if the fixed points were compatible with the processes being active. In that case, the Jacobian was evaluated at the equilibrium point to obtain the eigenvalues and assess the expected asymptotic equilibrium of each model, following standard practices (Strogatz 2015). The full analysis is included in the Supplementary Materials in Tables S1-S4.

Numerical simulations of the full model

The dynamic of the predator-prey model defined in Eq. 4 was obtained by integrating the system of differential equations using the *odeint* function in the Python's *scipy* library (Virtanen et al. 2020). This function solves a system of ordinary differential equations using the LSODA solver from

the FORTRAN library odepack (Hindmarsh 1983). The LSODA method automatically switches between nonstiff and stiff solvers depending on the behavior of the equations (Petzold 1983). The numerical simulations were performed for the four parameter scenarios discussed in the main text and listed in Model_results.csv. The final time was associated with the observational timescale in each scenario (see Results). The dimensionless weights of each process, critical times, and tipping points predicted by the FODAM method were obtained a posteriori. The times associated with crossing critical thresholds were extracted from the dynamic weights. The parameters, initial conditions, final conditions, and critical values and times of all simulated cases are in the supplementary file (Model_results.csv). To assess the robustness of the predictions from the FODAM method, additional simulations were performed, adding a carrying capacity term, $-B^2/K$, to the prey (bacteria) equation in Eq. 4. These simulations explored the four main scenarios. The relevant values for the simulation are also provided in the supplementary file (Model_results.csv).

Numerical simulation of the sequential simplified dynamics

The simplified model was obtained by programming a code in Python that switched to different models when crossing the tipping points. In each regime, the system was integrated with the *odeint* function from the *scipy* library as described in the previous paragraph. The simulations of the approximated sequential FODAM models were obtained for the four scenarios in the figures included in the results and supplementary material.

Colab

. The Colab notebook was developed using the FODAM approach. It was written in python and uses libraries *numpy*, *scipy*, and *google.colab* (Virtanen et al. 2020; Harris et al. 2020). The notebook simulates the dynamics of a given dynamical model, estimating the contribution (weight) of each process throughout the dynamics based on a specified observational time τ. The notebook takes the dynamic model and observational time as an input. The user can introduce the model manually or uploading a json file. In either case, the user needs to specify:

- Variables: names, symbols, units, inital values, and dependences.
- Parameters: names, symbols, units, and values.
- Processes or mechanisms: names and mathematical expressions.
- Observational time: value, variable, system size or volume, and units.

The notebook generates the simulated model as a json file (`dynamics_model.json`) and as a python file (`model_fun.py`) and a figure with the results (`dynamics_output.png`). The figure is a plot grid with the dynamics of each dependent variable (columns) and the weights of each process

(rows) directly impacting the rate of change of the dynamic variable. The notebook and repository are public:

Colab notebook: `https://colab.research.google.com/github/luquelab/dynamics/blob/main/dynamic_regimes.ipynb`

GitHub repository: `https://github.com/luquelab/dynamics`

Acknowledgements

The authors thank the invaluable insights from Joan Roughgarden and from the Biomath working group at San Diego State University and the insights from Alexander V. Alekseyenko (Medical University of South Carolina) for fruitful discussions at New York University that planted the seed of this project. The authors also acknowledge the crucial influence in the current study of the Master Thesis from Matt Witt carried under the supervision of Antoni Luque at San Diego State University (Witt 2019). The authors acknowledge the funding support of different agencies that made possible the research published here. The National Science Foundation award # 1951678 supported the research of A.L. The Gordon and Betty Moore Foundation, GBMF9871, grant https://doi.org/10.37807/GBMF9871 supported the research of A.L. and F.R. The Gordon and Betty Moore Foundation, GBMF9207, grant https://doi.org/10.37807/GBMF9207 supported the research of S.C.-L. and F.R. The Margarita Salas Grant for the training of young doctors 2021URV-MS-20 supported the research of S.C.-L..

References

I. Bashkirtseva and L. Ryashko. Stochastic sensitivity analysis of noise-induced extinction in the ricker model with delay and allee effect. *Bulletin of Mathematical Biology*, 80(6):1596–1614, 2018. doi: 10.1007/s11538-018-0422-6.

T. M. Bury et al. Deep learning for early warning signals of tipping points. *Proceedings of the National Academy of Sciences*, 118(39):e2106140118, 2021. doi: 10.1073/pnas.2106140118. URL `https://www.pnas.org/doi/abs/10.1073/pnas.2106140118`.

B. Cairns et al. Quantitative models of in vitro bacteriophage–host dynamics and their application to phage therapy. *PLoS Path.*, 5, 2009. doi: 10.1371/journal.ppat.1000253.

H. Cheng et al. Timing and structure of the younger dryas event and its underlying climate dynamics. *Proceedings of the National Academy of Sciences*, 117(38):23408–23417, 2020. doi: 10.1073/pnas.2007869117. URL `https://www.pnas.org/doi/abs/10.1073/pnas.2007869117`.

J. Cole and J. Kevorkian. Uniformly valid asymptotic approximations for certain non-linear differential equations1. In J. P. LaSalle and S. Lefschetz, editors, *International Symposium on*

Nonlinear Differential Equations and Nonlinear Mechanics, pages 113–120. Academic Press, 1963. ISBN 978-0-12-395651-4. doi: https://doi.org/10.1016/B978-0-12-395651-4.50018-0. URL https://www.sciencedirect.com/science/article/pii/B9780123956514500180.

D. Cushing et al. Moving toward an unstable equilibrium: saddle nodes in population systems. *Journal of Animal Ecology*, 67(2):298–306, 1998. doi: 10.1046/j.1365-2656.1998.00194.x.

K. De et al. An infrared transient from a star engulfing a planet. *Nature*, 617(7959):55–60, May 2023. ISSN 1476-4687. doi: 10.1038/s41586-023-05842-x. URL https://doi.org/10.1038/s41586-023-05842-x.

P. Ditlevsen and S. Ditlevsen. Warning of a forthcoming collapse of the atlantic meridional overturning circulation. *Nature Communications*, 14(1):4254, Jul 2023. ISSN 2041-1723. doi: 10.1038/s41467-023-39810-w. URL https://doi.org/10.1038/s41467-023-39810-w.

C. Folke et al. Resilience thinking: Integrating resilience, adaptability and transformability. *Ecology and Society*, 15(4), 2010. ISSN 17083087. URL http://www.jstor.org/stable/26268226.

C. R. Harris et al. Array programming with NumPy. *Nature*, 585(7825):357–362, September 2020. doi: 10.1038/s41586-020-2649-2. URL https://doi.org/10.1038/s41586-020-2649-2.

A. Hastings et al. Transient phenomena in ecology. *Science*, 361(6406):eaat6412, 2018. doi: 10.1126/science.aat6412. URL https://www.science.org/doi/abs/10.1126/science.aat6412.

W. B. Hayes. Is the outer solar system chaotic? *Nature Physics*, 3(10):689–691, Oct 2007. ISSN 1745-2481. doi: 10.1038/nphys728. URL https://doi.org/10.1038/nphys728.

A. C. Hindmarsh. Odepack, a systematized collection of ode solvers. *Scientific Computing, R. S. Stepleman et al. (eds.)*, 1:55–64., 1983.

J. Kevorkian and J. D. Cole. *Limit Process Expansions Applied to Ordinary Differential Equations*, pages 17–104. Springer New York, New York, NY, 1981. ISBN 978-1-4757-4213-8. doi: 10.1007/978-1-4757-4213-8_2. URL https://doi.org/10.1007/978-1-4757-4213-8_2.

J. Kevorkian. The two variable expansion procedure for the approximate solution of certain nonlinear differential equations. 1966.

J. Laskar and M. Gastineau. Existence of collisional trajectories of mercury, mars and venus with the earth. *Nature*, 459(7248):817–819, Jun 2009. ISSN 1476-4687. doi: 10.1038/nature08096. URL https://doi.org/10.1038/nature08096.

T. W. Lyons, C. T. Reinhard, and N. J. Planavsky. The rise of oxygen in earth's early ocean and atmosphere. *Nature*, 506(7488):307–315, Feb 2014. ISSN 1476-4687. doi: 10.1038/nature13068. URL https://doi.org/10.1038/nature13068.

L. Margulis and D. Sagan. *Microcosmos: Four Billion Years of Microbial Evolution*. Biology/Ecology/Environmental studies. University of California Press, 1997. ISBN 9780520210646. URL https://books.google.com/books?id=eo_sMMRxgAUC.

D. Oro et al. Social copying drives a tipping point for nonlinear population collapse. *Proceedings of the National Academy of Sciences*, 120(11):e2214055120, 2023. doi: 10.1073/pnas.2214055120. URL https://www.pnas.org/doi/abs/10.1073/pnas.2214055120.

S. Panahi, Y. Do, A. Hastings, and Y.-C. Lai. Rate-induced tipping in complex high-dimensional ecological networks. *Proceedings of the National Academy of Sciences*, 120(51):e2308820120, 2023. doi: 10.1073/pnas.2308820120. URL https://www.pnas.org/doi/abs/10.1073/pnas.2308820120.

E. J. Pedersen, M. Koen-Alonso, and T. D. Tunney. Detecting regime shifts in communities using estimated rates of change. *ICES Journal of Marine Science*, 77(4):1546–1555, 05 2020. ISSN 1054-3139. doi: 10.1093/icesjms/fsaa056. URL https://doi.org/10.1093/icesjms/fsaa056.

L. R. Petzold. Automatic selection of methods for solving stiff and nonstiff systems of ordinary differential equations. *Siam Journal on Scientific and Statistical Computing*, 4:136–148, 1983.

M. Rabinovich et al. Dynamical principles in neuroscience. *Reviews of Modern Physics*, 78(4): 1213–1265, 2006. doi: 10.1103/revmodphys.78.1213.

S. Rinaldi and M. Scheffer. Geometric analysis of ecological models with slow and fast processes. *Ecosystems*, 3(6):507–521, 2000. doi: 10.1007/s100210000045.

D. R. Roach et al. Synergy between the host immune system and bacteriophage is essential for successful phage therapy against an acute respiratory pathogen. *Cell Host & Microbe*, 22 (1):38–47.e4, 2017. ISSN 1931-3128. doi: https://doi.org/10.1016/j.chom.2017.06.018. URL https://www.sciencedirect.com/science/article/pii/S1931312817302585.

J. C. Rocha, G. Peterson, Örjan Bodin, and S. Levin. Cascading regime shifts within and across scales. *Science*, 362(6421):1379–1383, 2018. doi: 10.1126/science.aat7850. URL https://www.science.org/doi/abs/10.1126/science.aat7850.

M. Scheffer. *Critical Transitions in Nature and Society*. Princeton University Press, 2009. ISBN 9780691122045. URL http://www.jstor.org/stable/j.ctv173f1g1.

M. Scheffer et al. Early-warning signals for critical transitions. *Nature*, 461(7260):53–59, Sep 2009. ISSN 1476-4687. doi: 10.1038/nature08227. URL https://doi.org/10.1038/nature08227.

K.-P. Schroder and R. C. Smith. Distant future of the sun and earth revisited. 386(1):155–163, may 2008. doi: 10.1111/j.1365-2966.2008.13022.x. URL https://doi.org/10.1111%2Fj.1365-2966.2008.13022.x.

D. Seekell. Passing the point of no return. *Science*, 354(6316):1109–1109, 2016. doi: 10.1126/science.aal2188. URL https://www.science.org/doi/abs/10.1126/science.aal2188.

D. A. Seekell, S. R. Carpenter, and M. L. Pace. Conditional heteroscedasticity as a leading indicator of ecological regime shifts. *The American Naturalist*, 178(4):442–451, 2011. doi: 10.1086/661898. URL https://doi.org/10.1086/661898. PMID: 21956023.

D. A. Seekell, S. R. Carpenter, T. J. Cline, and M. L. Pace. Conditional heteroskedasticity forecasts regime shift in a whole-ecosystem experiment. *Ecosystems*, 15(5):741–747, 2012. ISSN 14329840, 14350629. URL http://www.jstor.org/stable/23253689.

D. A. Seekell, T. J. Cline, S. R. Carpenter, and M. L. Pace. Evidence of alternate attractors from a whole-ecosystem regime shift experiment. *Theoretical Ecology*, 6(3):385–394, Aug 2013. ISSN 1874-1746. doi: 10.1007/s12080-013-0183-7. URL https://doi.org/10.1007/s12080-013-0183-7.

S. Strogatz. *Nonlinear dynamics and chaos: with applications to physics, biology, chemistry, and engineering*. Westview Press, 2015.

P. Virtanen et al. Scipy 1.0: fundamental algorithms for scientific computing in python. *Nature Methods*, 17(3):261–272, Mar 2020. ISSN 1548-7105. doi: 10.1038/s41592-019-0686-2. URL https://doi.org/10.1038/s41592-019-0686-2.

M. C. Witt. *An Analytical Approach to Transient Dynamics: A Case Study on Phage and Bacteria Population Interactions*. PhD thesis, 2019. URL http://libproxy.sdsu.edu/login?url=https://www.proquest.com/dissertations-theses/analytical-approach-transient-dynamics-case-study/docview/2313671001/se-2. Copyright - Database copyright ProQuest LLC; ProQuest does not claim copyright in the individual underlying works; Última actualización - 2023-03-05.

Observed dynamics

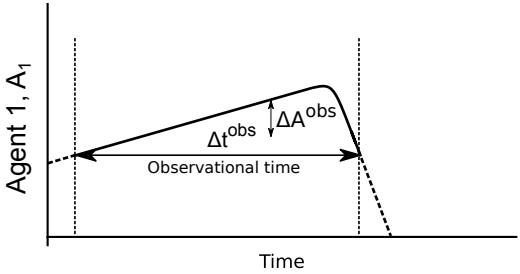

$$\underbrace{\frac{dA_1}{dt}}_{\text{Rate agent 1}} = \underbrace{F_{11}}_{\text{Process 1}} + \underbrace{F_{12}}_{\text{Process 2}}$$

Empirical factor $\dfrac{\Delta t^{obs}}{\Delta A_1^{obs}}$

$$\underbrace{\frac{\Delta t^{obs}}{\Delta A_1^{obs}}\frac{dA_1}{dt}}_{\text{Dimensionless rate}} = \underbrace{\frac{\Delta t^{obs}}{\Delta A_1^{obs}}F_{11}}_{\text{weight},w_{11}} + \underbrace{\frac{\Delta t^{obs}}{\Delta A_1^{obs}}F_{12}}_{\text{weight},w_{12}}$$

Active processes

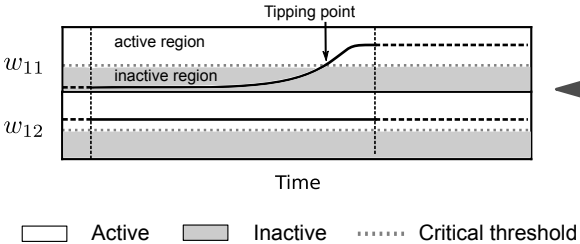

a)

$$\frac{dB}{dt} = \underbrace{rB}_{\text{Growth}} - \underbrace{aBP}_{\text{Predation}}$$

$$\frac{dP}{dt} = \underbrace{caBP}_{\text{Burst}} - \underbrace{mP}_{\text{Decay}}$$

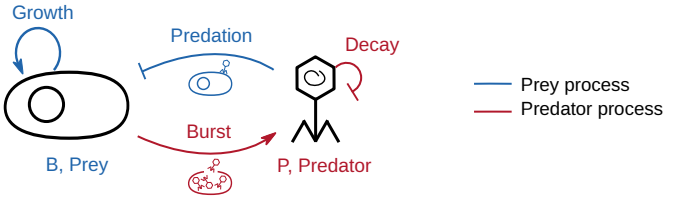

b)

Full
Simplified
Quasi-stable
Stable
Attractor = Att
Regime = R
sub-tipping point
G: Growth
B: Burst
P: Predation
D: Decay
t_0 Initial time
t_f Final time

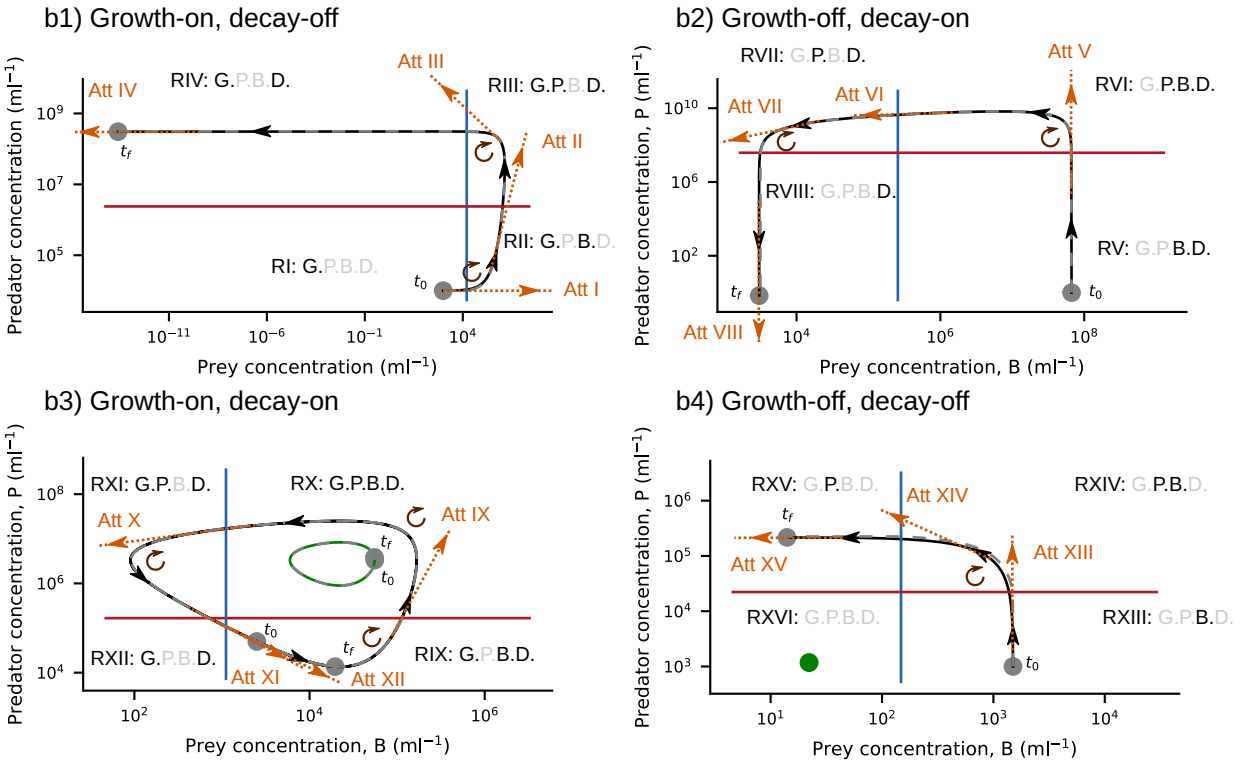

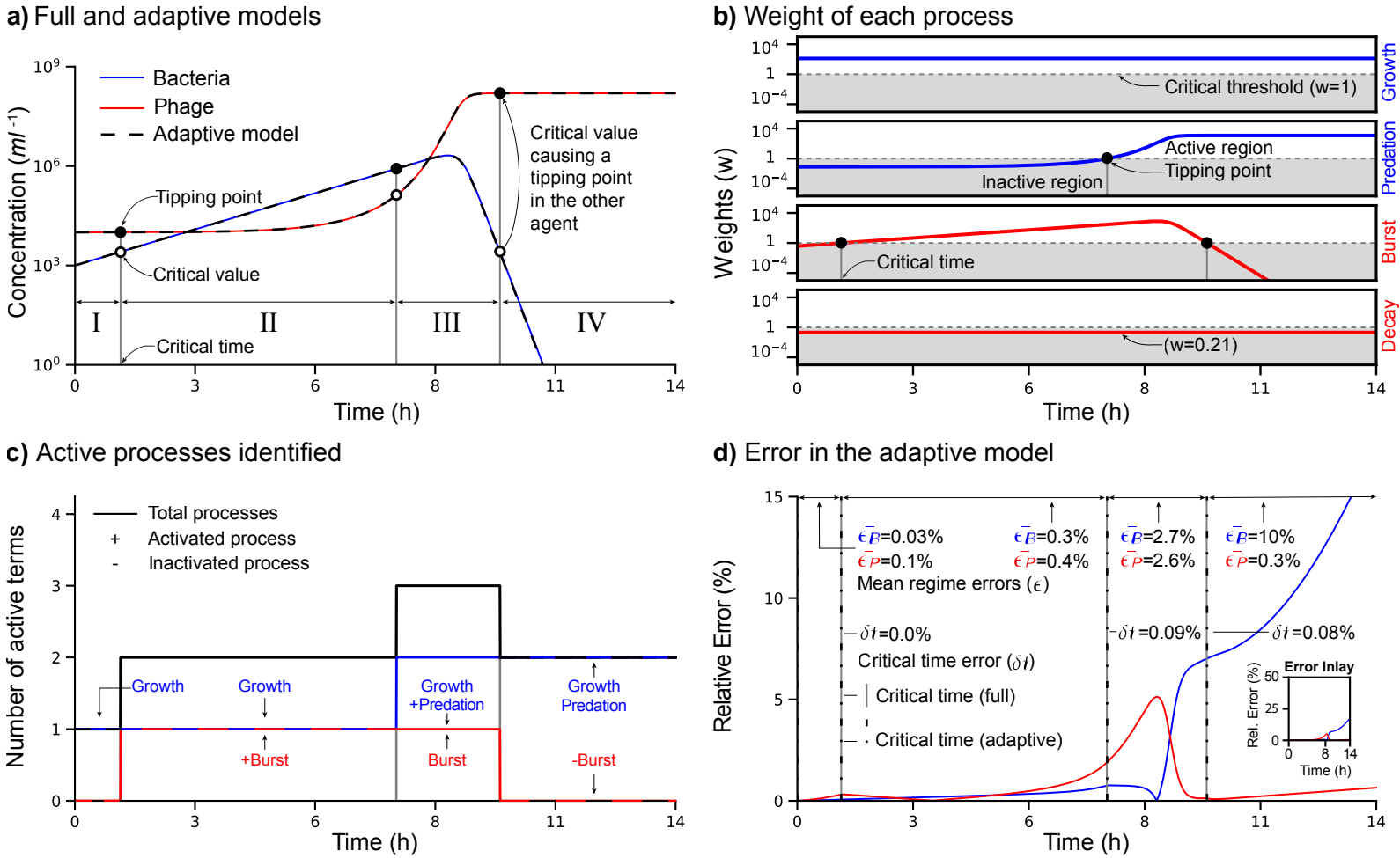
a) Full and adaptive models
Bacteria
Phage
Adaptive model
Concentration (ml⁻¹)
Tipping point
Critical value
Critical value causing a tipping point in the other agent
Critical time
I
II
III
IV
Time (h)
b) Weight of each process
Weights (w)
Critical threshold (w=1)
Growth
Active region
Tipping point
Inactive region
Predation
Critical time
Burst
(w=0.21)
Decay
Time (h)
c) Active processes identified
Total processes
Activated process
Inactivated process
Number of active terms
Growth
Growth
+Burst
Growth +Predation
Burst
Growth Predation
-Burst
Time (h)
d) Error in the adaptive model
Relative Error (%)
ε̄B=0.03%
ε̄P=0.1%
ε̄B=0.3%
ε̄P=0.4%
ε̄B=2.7%
ε̄P=2.6%
ε̄B=10%
ε̄P=0.3%
Mean regime errors (ε̄)
δt=0.0%
δt=0.09%
δt=0.08%
Critical time error (δt)
Critical time (full)
Critical time (adaptive)
Error Inlay
Rel. Error (%)
Time (h)
Time (h)

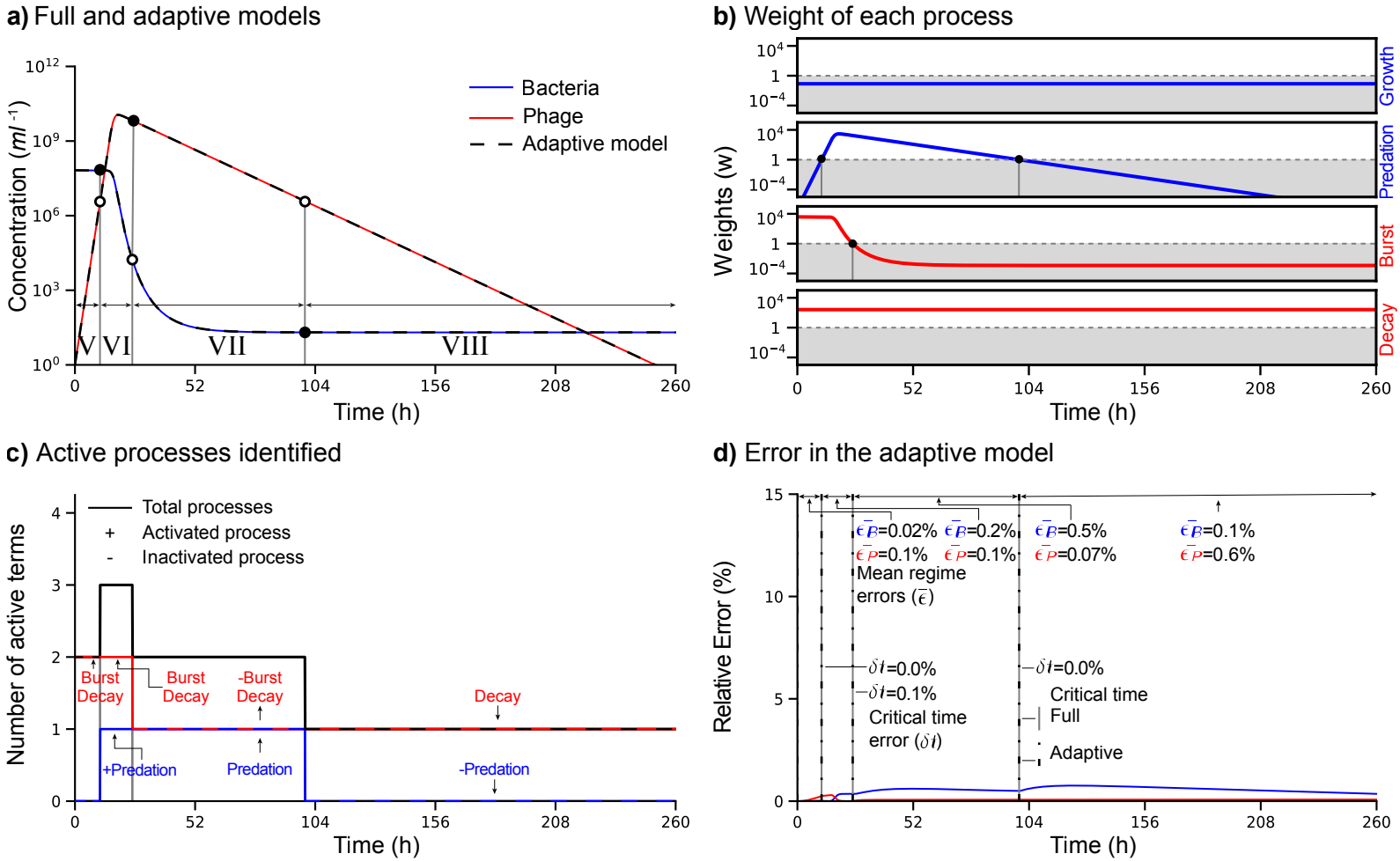
a) Full and adaptive models
Concentration (ml⁻¹)
Bacteria
Phage
Adaptive model
V VI VII VIII
Time (h)
b) Weight of each process
Weights (w)
Growth
Predation
Burst
Decay
Time (h)
c) Active processes identified
Number of active terms
Total processes
+ Activated process
- Inactivated process
Burst Decay
Burst Decay
-Burst Decay
Decay
+Predation
Predation
-Predation
Time (h)
d) Error in the adaptive model
Relative Error (%)
ε̄B=0.02% ε̄B=0.2% ε̄B=0.5% ε̄B=0.1%
ε̄P=0.1% ε̄P=0.1% ε̄P=0.07% ε̄P=0.6%
Mean regime errors (ε̄)
δt=0.0%
δt=0.1%
Critical time error (δt)
δt=0.0%
Critical time
Full
Adaptive
Time (h)

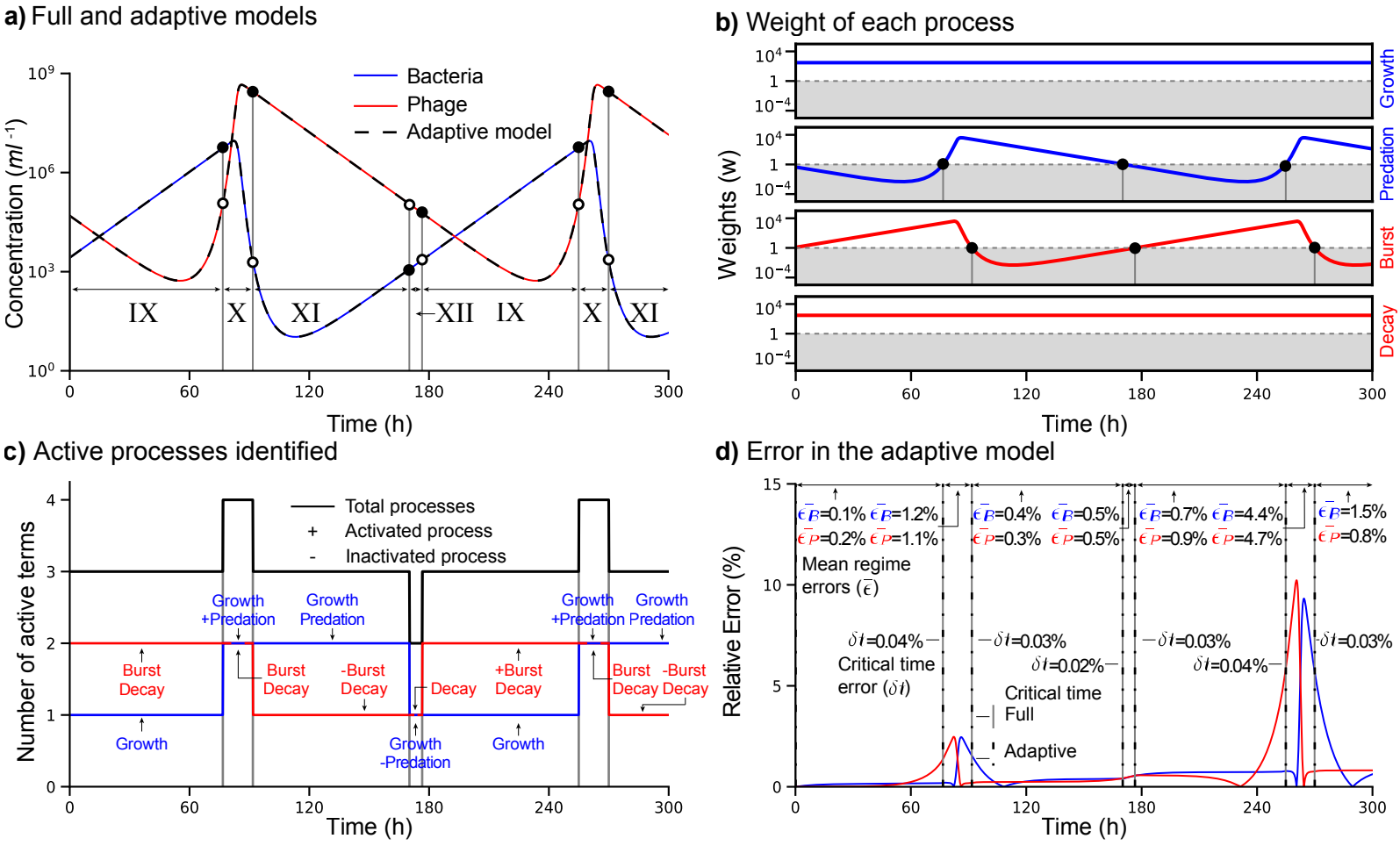
a) Full and adaptive models
Bacteria
Phage
Adaptive model
Concentration (ml⁻¹)
IX
X
XI
XII
IX
X
XI
Time (h)
b) Weight of each process
Weights (w)
Growth
Predation
Burst
Decay
Time (h)
c) Active processes identified
Total processes
+ Activated process
- Inactivated process
Number of active terms
Growth +Predation
Growth Predation
Burst Decay
Growth
Burst Decay
-Burst Decay
Growth -Predation
Decay
+Burst Decay
Growth
Growth +Predation
Growth Predation
Burst Decay
-Burst Decay
Time (h)
d) Error in the adaptive model
Relative Error (%)
Mean regime errors (ϵ̄)
ϵ̄B=0.1% ϵ̄B=1.2%
ϵ̄P=0.2% ϵ̄P=1.1%
ϵ̄B=0.4% ϵ̄B=0.5%
ϵ̄P=0.3% ϵ̄P=0.5%
ϵ̄B=0.7% ϵ̄B=4.4%
ϵ̄P=0.9% ϵ̄P=4.7%
ϵ̄B=1.5%
ϵ̄P=0.8%
Critical time error (δt)
δt=0.04%
δt=0.03%
δt=0.02%
δt=0.03%
δt=0.04%
δt=0.03%
Full
Adaptive
Time (h)